Materials Science & Engineering A 631 (2015) 120–125

Contents lists available at ScienceDirect

Materials Science & Engineering A

journal homepage: www.elsevier.com/locate/msea

Investigation of Portevin – Le Chatelier effect in HT-9 steel

Apu Sarkar [a,*], Sturat A. Maloy [b], Korukonda L. Murty [a]

[a] Department of Nuclear Engineering, North Carolina State University, Raleigh, NC 27695, USA
[b] Los Alamos National Laboratory, Los Alamos, NM 87545, USA

ARTICLE INFO

Article history:
Received 13 November 2014
Accepted 8 February 2015
Available online 24 February 2015

Keywords:
Portevin – Le Chatelier effect
Dynamic strain aging
HT-9 steel
Tensile tests

ABSTRACT

Portevin – Le Chatelier (PLC) effect has been observed in HT-9 steel. The present study involves different types of tensile testing to characterize the features of PLC effectin HT-9 steel. Stress serrations observed during tensile tests are analyzed using different statistical analysis techniques to investigate the underlying nature of the effect. Peaked type of stress drop distribution indicated occurrence of type B serrations in the steel. Multiscale entropy analysis of the stress serrations indicated substitutional solute atoms to be responsible for the PLC effect in HT-9 steel.

1. Introduction

The Portevin – Le Chatelier effect (PLC effect) is a type of plastic instability observed in many dilute alloys when they undergo plastic deformation [1–8]. This phenomenon is observed in a certain range of temperatures and strain-rates and consists in the deformation being inhomogeneous, dominated by successive strain localization events. At a certain value of the plastic strain known as the critical strain, the character of the deformation changes from homogeneous to inhomogeneous, which is indicated by the occurrence of serrations on the stress – strain curve which ultimately leads to band-type macroscopic surface markings. These limit the potential application of material when good surface quality is required. Moreover, PLC effect is associated with degradation of mechanical properties [9–13]. like loss of ductility and decrease in fracture toughness, reduction in fatigue life which makes it of concern to engineers. The physical origin of the PLC effect is attributed to dynamic strain aging (DSA) [1–8], a generic term representing a host of small-scale phenomena associated with the interaction of dislocations and solute atoms. DSA leads to the negative strain rate sensitivity (SRS) [7,8,14–16]. In fact, the PLC effect is a direct manifestation of the negative SRS, which gives rise to material instability. The ratio of the flow stress variation corresponding to an imposed strain rate variation is the measure of the SRS. If this becomes negative, conditions exist for the macroscopic observation of the PLC effect.

In the last few decades several studies have been carried out on the PLC effect and several models have also been proposed [17–33]. The first model was due to Cottrell [34]. which is based on the pinning and unpinning of dislocations by the solute atoms. In this model the basic assumption is that the solute atoms have sufficient mobility to follow the dislocations as they move continuously through the lattice. This process leads to an increased friction force for mobile dislocations. It was later realized [7] that solute atoms do not have sufficient mobility to follow moving dislocations and aging should take place while dislocations are arrested at obstacles such as at forest dislocations. Van den Beukel [3]. developed this idea into a quantitative model of DSA. The basic mechanism envisioned is clustering of the solute atoms at the mobile dislocations temporarily arrested at the obstacles through the bulk diffusion or by pipe diffusion. Dislocations overcome the barrier by the aid of thermal activation and jump to the next obstacles at high velocity.

Apart from these theoretical studies the PLC effect has also been a topic of several experimental investigations in the last few decades [17,23,35–40]. The PLC effect is most conveniently studied through tensile tests either at constant applied stress rate (‘soft’device) or at constant strain rate (‘hard’ device) within certain ranges of the control variables (stress and strain rate) and deformation temperature. In uniaxial loading with a constant imposed strain rate, the effect manifests itself as serrations in the stress – time (or strain) curves. This is associated with the repeated generation and propagation of plastic deformation bands. The bands mark the region of appreciable plastic deformation. Each stress drop is associated with the nucleation of a band of localized plastic deformation.

In polycrystals three types of the PLC effect are traditionally distinguished on the qualitative basis of the spatial arrangement of localized deformation loads and the particular appearance of deformation curves [32,41]. Three generic types of serrations: types A, B and C occur depending on the imposed cross-head velocity, i.e. strain rate. For sufficiently large strain rate, type A serrations are observed. In this case, the bands propagate continuously and are highly correlated. The associated stress drops are small in amplitude [31,33,42–47]. If the strain rate is lowered, type B serrations with

* Corresponding author. Tel.: +1 9195619244.
E-mail addresses: asarkar5@ncsu.edu, apusarkar@gmail.com (A. Sarkar).

http://dx.doi.org/10.1016/j.msea.2015.02.022
0921-5093/

relatively larger amplitude occur around the uniform stress – strain curve. These serrations correspond to intermittent band propagation. The deformation bands are formed ahead of the previous one in a spatially correlated manner and give rise to regular surface markings [31,33,42–47]. For even lower strain rate, bands become static. This type C band nucleates randomly in the sample leading to large saw-tooth shaped serrations in the stress – strain curve and random surface markings [31,33,42–47].

The PLC effect has been extensively studied over the last several decades with the goal being to achieve a better understanding of the small-scale processes and of the multiscale mechanisms that link the mesoscale DSA to the macroscale PLC effect. The technological goal is to increase the SRS to positive values in the range of temperatures and strain-rates relevant for industrial processes. This would ensure material stability during processing and would eliminate the occurrence of the PLC effect.

Ferritic/martensitic (F/M) steels are considered to be potential candidate materials for the core structural material of fast reactors (FRs), and also for the blanket and first wall materials of fusion reactors because of their superior swelling resistance [48–53]. HT-9 is a typical F/M steel which has been investigated extensively considering its prospective use in the nuclear industry [53–59]. HT-9 is also called a 12Cr-1MoVW steel. It has high chromium (Cr) content of about 12% and thus HT-9 is also called a high-chromium F/M steel. Presence of increased Cr content in this steel provides excellent resistance to atmospheric corrosion and resistance to degradation in many organic media. The presence of molybdenum (Mo) enhances the localized corrosion resistance in environments containing deleterious species by preventing the breakdown of protective oxide films. HT-9 steel has a body-centered-cubic (BCC) structure which gives better swelling resistant property in comparison with austenitic stainless steels.

2. Experimental details

HT-9 material used in this study was received in the form of as cast and rolled plates. The chemical composition of HT-9 steel is shown in Table 1. Tensile specimens of 10 mm gauge length and 0.5 mm thickness were machined along the rolling direction from the rolled plate and Fig. 1 shows the Transmission Electron Micrograph (TEM) of the as-received sample. The material is composed of elongated grains along the rolling direction. Tensile tests have been utilized in this study to investigate the PLC effect in the HT 9 steel. Uniaxial constant strain rate tensile tests, strain rate change tests and stress relaxation tests were carried out in the temperature range of 25 to 400 °C at strain-rates 10^{-3} and $10^{-4}\ s^{-1}$ using an INSTRON (model 1152) machine. A three zone furnace was used to heat the sample. A thermocouple was attached to the sample to monitor the temperature. Load and displacement recorded during the tensile tests were converted to stress (σ) and strain (ε) using conventional formulae.

3. Results and discussions

3.1. Tensile test, strain rate change test and stress relaxation test

Fig. 2 shows the engineering stress – strain curves of HT-9 steel for different deformation conditions. Serrations are visible in the

Table 1
Chemical composition of the HT-9 steel.

Cr	Ni	W	Mo	Mn	Si	V	C	Fe
11.94	0.62	0.48	1.03	0.6	0.30	0.30	0.21	Balance

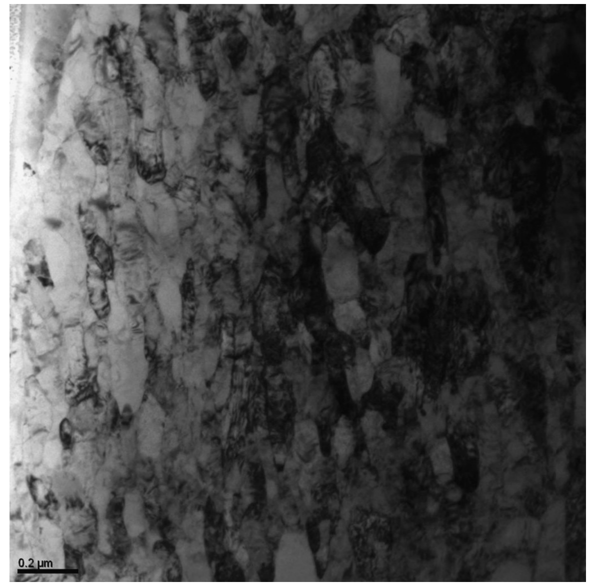

Fig. 1. Microstructure of the HT-9 steel used in the present study showing elongated grains along rolling direction.

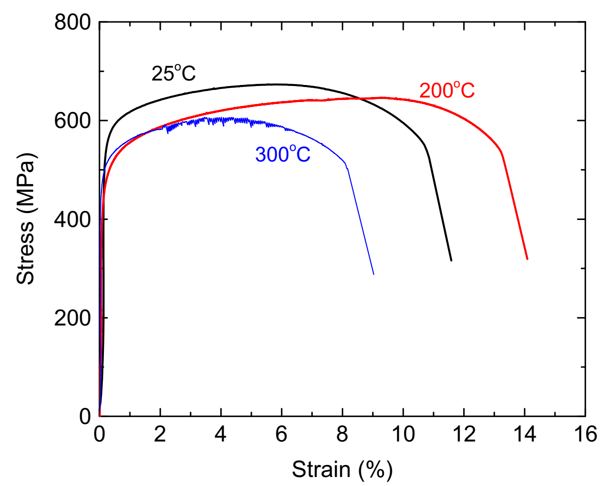

Fig. 2. Engineering stress – strain curves of HT-9 steel obtained from tensile tests at three different temperatures for strain-rate of $10^{-4}\ s^{-1}$.

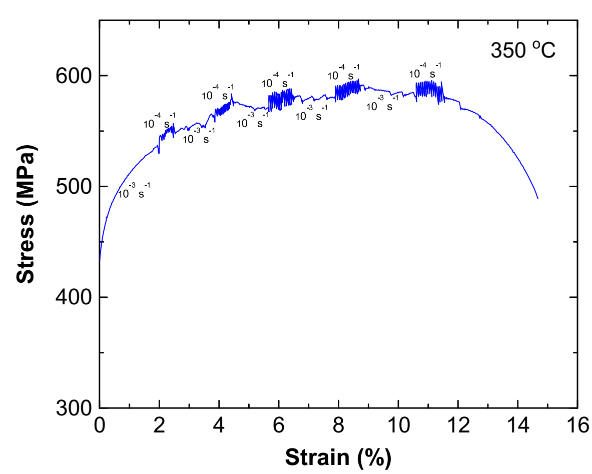

Fig. 3. Stress – strain curves of HT-9 steel obtained during strain rate jump test at 350 °C.